Retrieval of aerosol refractive index from extinction spectra with a damped harmonic-oscillator band model

Gareth E. Thomas, Stephen F. Bass, Roy G. Grainger, and Alyn Lambert

A new method for the retrieval of the spectral refractive indices of micrometer-sized particles from infrared aerosol extinction spectra has been developed. With this method we use a classical damped harmonic-oscillator model of molecular absorption in conjunction with Mie scattering to model extinction spectra, which we then fit to the measurements using a numerical optimal estimation algorithm. The main advantage of this method over the more traditional Kramers–Kronig approach is that it allows the full complex refractive-index spectra, along with the parameters of the particle size distribution, to be retrieved from a single extinction spectrum. The retrieval scheme has been extensively characterized and has been found to provide refractive indices with a maximum uncertainty of ~10% (with a minimum of ~0.1%). Comparison of refractive indices calculated from measurements of a ternary solution of HNO_3, H_2SO_4, and H_2O with those published in J. Phys. Chem. A **104**, 783 (2000) show similar differences as found by other authors. © 2005 Optical Society of America

OCIS codes: 120.4530, 290.2200, 300.6340, 350.4990.

1. Introduction

Remote sensing of the atmosphere with mid-infrared radiometers and spectrometers—from satellites, aircraft, and ground-based platforms—is one of the primary tools used to determine atmospheric composition. Recent years have seen this measurement technique play an increasingly important role in the determination of the composition, volume, phase, and size of stratospheric aerosol.[1] Knowledge of the aerosol's refractive index is of key importance to determine the accuracy of retrieved aerosol parameters from such measurements.

The primary aerosols found in the stratosphere are composed of sulphuric acid solution or, in the case of polar stratospheric clouds, ternary solutions of H_2SO_4, HNO_3, and water. Therefore, to improve the accuracy of satellite-based measurements of stratospheric aerosol, many laboratory-based measurements of H_2SO_4 and HNO_3 binary[2–5] and H_2SO_4 and HNO_3 ternary solution[6,7] refractive indices have been made in recent years. These measurements have shown that the refractive index is not only strongly dependent on aerosol composition, but also on temperature because of the temperature-dependent ion equilibrium in the sulphuric and nitric acid systems. This increases the need for optical constants of an aqueous sulphuric and nitric acid aerosol to be measured across a broad range of stratospherically relevant temperatures and compositions.

Although current laboratory data have undoubtedly improved the accuracy of refractive indices used in the analysis of mid-infrared atmospheric measurements, there remain significant differences between the individual data sets.[8] In particular, most available refractive indices thus far have been derived from spectral measurements of thin films. McPheat *et al.*[9] showed that there are significant differences in extinction spectra resulting from thin films and those from aerosol. Although some measurements of aerosol-based refractive indices are available, they cover a narrow range of compositions.

One reason for the lack of laboratory measurements of aerosol spectra is that determination of refractive index from aerosol measurement is significantly more difficult than for thin-film measurements. The traditional way to determine the refractive index from extinction measurements is to

When this research was performed, G. E. Thomas (gthomas@atm.ox.ac.uk), S. F. Bass, and R. G. Grainger were with the Sub-Department of Atmospheric, Oceanic and Planetary Physics, Clarendon Laboratory, University of Oxford, Parks Road, Oxford OX1 3PU, UK. S. F. Bass is now with the Science Strategy Team, Department for Environment Food and Rural Affairs, Cromwell House, Dean Stanely Street, London SW1P 3JH, UK. A. Lambert is with the Division of Atmospheric Chemistry, National Center for Atmospheric Research, P.O. Box 3000, Boulder, Colorado 80307-3000.

Received 4 June 2004; revised manuscript received 29 October 2004; accepted 3 November 2004.

0003-6935/05/071332-10$15.00/0

© 2005 Optical Society of America

employ the Kramers–Kronig relation between the real and the imaginary parts of the refractive index (see, for example, Clapp *et al.*,[10] Niedziela *et al.*,[3] Biermann *et al.*[6]). The major disadvantage of this approach when applied to aerosol measurements is that, to gain absolute spectral refractive indices, two extinction spectra are required for each composition and temperature combination.[10] It is therefore necessary to measure spectra for two separate particle size distributions, without altering either particle composition or ambient temperature. In the case of volatile liquid aerosol, this presents significant experimental difficulties. In addition, Wagner *et al.*[8] suggest that, if the initial guess at the spectral refractive indices is not sufficiently accurate, the analysis will result in incorrect results.

In this paper we present a method for determining complex spectral refractive indices, as well as size distribution parameters, from a single infrared aerosol extinction spectrum. With this method, pioneered by Bass,[11] we use a classical damped harmonic-oscillator (CDHO) model of molecular absorption,[12] along with a Mie-scattering algorithm, to predict aerosol extinction. The modeled extinction is then fitted to measurements with a numerical retrieval scheme. This approach removes the necessity of making two distinct measurements of aerosol with the same composition and thus greatly simplifies the experimental requirements for the determination of aerosol refractive indices.

2. Retrieval Method

The determination of aerosol optical properties from measurements of extinction spectra is an example of a retrieval problem that is amenable to the application of numerical optimization techniques. If we define a measurement vector $\mathbf{y}$ consisting of the measured extinction values, with an associated error covariance matrix $\mathbf{S}_\epsilon$, the retrieval problem can be expressed in terms of finding the value of the state vector $\mathbf{x}$ for which the forward model $\mathbf{F}(x)$ produces the best fit to $\mathbf{y}$, subject to the constraints imposed by any prior knowledge we have of the state.

The algorithm used to perform the retrieval is the Levenberg–Marquardt method, and the quality of the fit between the state estimate and the measurement is measured by the conditional probability of the state given the measurement $P(\mathbf{x}|\mathbf{y})$:

$$-2 \ln P(\mathbf{x}\,|\,\mathbf{y}) = [\mathbf{y} - \mathbf{F}(\mathbf{x})]^T \mathbf{S}_\epsilon^{-1} [\mathbf{y} - \mathbf{F}(\mathbf{x})] + (\mathbf{x} - \mathbf{x}_a)^T \mathbf{S}_a^{-1} (\mathbf{x} - \mathbf{x}_a). \quad (1)$$

Here $\mathbf{x}_a$ represents our best estimate of the state before the measurement was made (the *a priori*) and $\mathbf{S}_a$ is its covariance matrix representing the uncertainty in this knowledge. The quantity defined in Eq. (1) is the function minimized by the retrieval algorithm (the cost function) and is essentially the sum of squares of the differences between the measurement and the forward model and between the state estimate and the *a priori* measurement, weighted by the measurement and *a priori* uncertainties, respectively.

Details of the numerical optimal estimation and the Levenberg–Marquardt technique have been widely published (see Press *et al.*[13] and Rodgers,[14] for example).

3. Forward Model

The heart of this analysis scheme is the forward model, which maps the state vector to a corresponding measurement vector. With the technique described here, we use a CDHO model of molecular absorption to relate physical properties of a substance to its refractive index at a given wavelength. This refractive index is then used by a Mie-scattering algorithm to predict the extinction that results from a distribution of particles of the given type.

The CDHO model relates the wavelength-dependent complex molar polarizability, $\alpha_m(\nu) = \alpha_m'(\nu) + i\alpha_m''(\nu)$, to a set of p vibration bands, with each band being described by the oscillator's central wave number ν_j, width (damping constant) γ_j, and intensity S_j, where $j = 0, 1, \ldots, p$, by the relations[12]

$$\alpha_m'(\nu) = \frac{3N_A(\epsilon_\infty - 1)}{4\pi N(\epsilon_\infty + 2)} + \frac{N_A}{4\pi^2 c^2} \sum_j \frac{(\mu_j^2/3)(\nu_j^2 - \nu^2)}{(\nu_j^2 - \nu^2)^2 - \gamma_j^2 \nu^2}, \quad (2)$$

$$\alpha_m''(\nu) = \frac{N_A}{4\pi^2 c^2} \sum_j \frac{(\mu_j^2/3)\gamma_j \nu}{(\nu_j^2 - \nu^2)^2 - \gamma_j^2 \nu^2}, \quad (3)$$

where N_A is Avogadro's number, μ_j is the derivative of the dipole moment with respect to the normal coordinate for the jth band (and is divided by three to account for the random orientation of molecules in the sample), N is the number of molecules in a unit volume, and ϵ_∞ is the value the dielectric constant takes at an infinite wavelength (zero frequency).

Note that from Eqs. (2) and (3), determination of $\alpha(\nu)$ is not possible without knowledge of N and μ_j. However, using the Lorentz–Lorenz relation,

$$\frac{\epsilon(\nu) - 1}{\epsilon(\nu) + 2} = \frac{m(\nu)^2 - 1}{m(\nu)^2 + 2} = \frac{4}{3} \pi N \alpha(\nu), \quad (4)$$

where N is the number of molecules per unit volume, we can relate the real and imaginary parts of the complex dielectric constant for a material [$\epsilon'(\nu)$ and $\epsilon''(\nu)$, respectively] to the band parameters:[12]

$$\epsilon'(\nu) = \epsilon_\infty + \sum_j \frac{S_j(\nu_j^2 - \nu^2)}{(\nu_j^2 - \nu^2)^2 + \gamma_j^2 \nu^2}, \quad (5)$$

$$\epsilon''(\nu) = \sum_j \frac{s_j \gamma_j \nu}{(\nu_j^2 - \nu^2)^2 + \gamma_j^2 \nu^2}. \quad (6)$$

Note that Eq. (4) differs from the usual form of the Clausius–Mossotti equation in that ϵ, m, and α are all

wavelength-dependent, complex quantities. The inclusion of complex quantities in Eq. (4) accounts for absorption features within a spectrum.

Finally, the refractive and absorptive components of the complex refractive index ($m = n + ik$) can also be calculated, again from application of Eq. (4):

$$n(\nu) = \left(\frac{\left\{ \left[\epsilon'(\nu)^2 + \epsilon''(\nu)^2 \right]^{1/2} + \epsilon'(\nu) \right\}}{2} \right)^{1/2}, \tag{7}$$

$$k(\nu) = \left(\frac{\left\{ \left[\epsilon'(\nu)^2 + \epsilon''(\nu)^2 \right]^{1/2} - \epsilon'(\nu) \right\}}{2} \right)^{1/2}. \tag{8}$$

As an aside, we also note that

$$\alpha_m{}'(\nu) = \frac{3N_A}{4\pi N} \frac{[\epsilon'(\nu) - 1][\epsilon'(\nu) + 2] + \epsilon''(\nu)^2}{[\epsilon'(\nu) + 2]^2 + \epsilon''(\nu)^2}, \tag{9}$$

$$\alpha_m{}''(\nu) = \frac{9N_A}{4\pi N} \frac{\epsilon''(\nu)}{[\epsilon'(\nu) + 2]^2 + \epsilon''(\nu)^2}. \tag{10}$$

Thus, given knowledge of N, the molar polarizability can be computed without knowledge of μ_j. Although this parameter is not currently included in the output of the forward model, accurate knowledge of particle composition would allow it to be calculated in addition to the refractive index.

It should be noted that the CDHO model relies on the assumption that each individual oscillator j is sufficiently isolated so that the dielectric constant due to all other oscillators is real and constant across the frequency range of oscillator j. In practice, despite its approximation of the physical process of molecular absorption, the CDHO model produces α_m absorption bands that are extremely close to those observed,[12] provided that the features are symmetric. In addition, the Lorenz field, which allows the application of Eq. (4), is valid only for isotropic materials with close to spheric geometry in which the constituent molecules are small in comparison to the wavelength of the radiation causing the excitation.[15] Most ionic liquids, light hydrocarbons, and many solids satisfy these criteria, however.

The forward model uses Eqs. (5)–(8) to calculate spectral refractive indices for a given band parameter set. The $\epsilon_\infty = m_\infty{}^2$ parameter is included as a fixed parameter, based on relevant published values of refractive index at visible wavelengths.

These refractive indices are then used to calculate the extinction of the aerosol population with a Mie-scattering algorithm and an assumed form of particle size distribution. The most common size distribution, particularly for liquid aerosol, is log normal; and it is this form that we use as an example. With these assumptions, it is the band parameters (ν_j, γ_j, and S_j) along with the parameters describing the size distribution that provide the input for the forward model and thus form the state vector for the retrieval problem. The total extinction, at a wave number ν, of an aerosol population with a log-normal size distribution is

$$\beta^{\text{ext}}(\nu) = \frac{N_0}{\ln S} \sqrt{\frac{\pi}{2}} \int_0^\pi r Q^{\text{ext}}(\nu,\ m,\ r) \times \exp\left[-\frac{(\ln r - \ln r_m)^2}{2 \ln^2 S} \right] dr, \tag{11}$$

where r_m is the median radius of the distribution and the standard deviation of $\ln r$ is $\ln S$; N_0 is the total number density of particles; and $Q^{\text{ext}}(\nu,\ m,\ r)$ is the extinction efficiency of a particle of radius r, as given by Mie-scattering theory. Thus the state vector used in the retrievals consists of N_0, r_m, S, and p sets of the three band parameters (ν_j, γ_j, and S_j), where, to describe a typical infrared aerosol extinction spectrum, $p \lesssim 50$. Determining the exact number of bands required to fit a given spectrum is in itself a difficult problem. Ideally, measurements of the infrared absorption features of the component compounds making up the aerosol of interest would be used to define the *a priori* band set. Unfortunately, in practice there are a lack of such measurements in the literature, and thus building the *a priori* band set must be done in a more *ad hock* fashion. Thus far the method employed has been to build the best possible set from knowledge of the expected absorption bands of the material in question and then add and remove bands based on the results of trial retrieval runs. For example, if a feature present in the measured spectra is consistently missing in the retrieved spectra, a band is added to improve the fit. Conversely, if the retrieval algorithm consistently returns a low strength (S_j) for a particular band, it is removed as it is not required to fit the spectra. Although this approach has been found to provide excellent spectral fits, the uncertainty in the *a priori* band structure still represents a significant systematic error in the forward model.

An additional feature of this forward model is that all derivatives (which are a vital component of the retrieval process since they make up the Jacobians) are calculated analytically. Use of analytical derivatives results in both an increase in the accuracy of the derivative values and a considerable saving in computation time (since the forward model need be computed only once for each state estimate, rather than the many times required to compute numerical derivatives by perturbing each state element in turn). Grainger *et al.*[16] give expressions for the derivatives of Mie-scattering functions with respect to refractive index, as well as the parameters of a log-normal size distribution. The derivatives of refractive index with respect to the band parameters, as well as the process by which the different derivatives are combined to form the Jacobians, are detailed in Appendix A.

4. Implementation of the Retrieval Algorithm

Use of the CDHO and Mie forward models in this retrieval problem introduces two complicating factors in the representation of the state and the final solution. First, as we are not directly retrieving the quantity of interest (i.e., the complex refractive index of the particles), but rather the CDHO band parameters that best reproduce the measured spectra, the characterization of the solution is more complicated than in the standard case. Second, the elements of the state vector have a range of values that cover several orders of magnitude, as does the forward model's sensitivity to these elements.

We addressed the first of these issues by applying a cutdown version of the forward model that calculates the refractive index from the band parameters without performing the Mie-scattering calculations to the solution. This calculation can be represented by the equation

$$\mathbf{m} = \mathbf{f}_m(\mathbf{x}), \tag{12}$$

where $\mathbf{m}$ is a vector of complex refractive indices, $\mathbf{x}$ is the state vector containing the CDHO band parameters, and $\mathbf{f}_m$ represents the cutdown forward model.

The second issue causes numerical instabilities during the retrieval process, particularly with the inversion of the covariance matrices, which in turn results in inaccurate error estimates. To prevent this, the logarithm of the state vector is retrieved, rather than the state itself. In addition to reducing numerical instabilities, retrieval in log space has the added advantage that it constrains all elements of the state vector to be positive (which corresponds to the physical constraints).

5. Error Propagation

In addition to an estimate of the spectral refractive indices (our state estimate), we required a characterization of the precision of these estimates. Optimal estimation provides error estimates in the retrieved state based on the uncertainties in the measurement, *a priori*, and forward model. The sources of error that need to be taken into account in the retrieval of the refractive index with the CDHO and Mie models are

1. measurement noise;
2. the uncertainty in *a priori* information;
3. errors due to assumptions made in the forward model and due to its approximate nature (i.e., taking into account that the model does not accurately represent the true physical processes taking place in molecular absorption); and
4. the uncertainty in forward model parameters, most notably m_∞.

The standard formulation for the optimal estimation of the expected value of the state explicitly includes the measurement noise and *a priori* uncertainty in the form of the measurement and *a priori* covariance matrices. The measurement covariance accounts for the measurement noise, and the *a priori* covariance essentially defines the region of state space where acceptable solutions can lie.

Important sources of error in a retrieval scheme are inaccuracies within the forward model, particularly when the model is a simplification of the physical processes, as is the case with the CDHO model. Here, this forward model error is due to both the approximate nature of the CDHO model and the assumptions inherent in the Mie-scattering model. A significant source of error in the CDHO forward model originates from the poor prior knowledge of the absorption bands expected for a given species. There have been relatively few measurements to determine the number, frequency, and strength of individual absorption features that make up the absorption spectra of species commonly found in atmospheric aerosol. It is thus not possible to provide a well-constrained set of band parameters to the retrieval—the only criteria for an acceptable band set is its ability to model the observed extinction spectra. However, it has been found that if an inaccurate band set is used, even though it might provide an excellent fit to an extinction spectrum, the discrepancy between the retrieved and the true spectral refractive indices will generally be greater than that predicted by retrieval error estimates.

In addition to errors resulting from the CDHO part of the forward model, errors due to the Mie-scattering model must also be taken into account. The two main assumptions inherent in the Mie-scattering model used here are that the particles are spherical and that they conform to a given size distribution. In many experimental cases these assumptions will be quite accurate—particularly if the aerosol is liquid and independent measurements of the size distribution are made. However, if solid particles, such as ice or mineral dust, were to be analyzed, it is likely that the accuracy of the forward model would be substantially reduced. This is particularly true of mineral dust samples, which, in addition to being nonspherical, often have multimodal size distributions.

To characterize forward model error terms such as these, an ensemble of retrievals based on a measurement of a known state must be performed. The expectation value of the squared difference between the true and the retrieved states, mapped onto measurement space, will provide the covariance matrix for the forward model error:

$$\mathbf{S}_{\mathrm{fm}} = \epsilon\{[\mathbf{K}(\mathbf{x} - \hat{\mathbf{x}})][\mathbf{K}(\mathbf{x} - \hat{\mathbf{x}})]^T\}, \tag{13}$$

where $\mathbf{K}$ is the Jacobian matrix (made up of the derivatives calculated by the forward model) that maps the true state onto the measurement, $\mathbf{x}$ denotes the true state, and $\hat{\mathbf{x}}$ denotes the retrieved state. This covariance is then used to modify the weighting introduced by the measurement error by simple addition:

$$\mathbf{S}_y = \mathbf{S}_\epsilon + \mathbf{S}_{\mathrm{fm}}. \tag{14}$$

In practice this calculation requires either a sequence of measurements of a known aerosol or the errors estimated by performing a series of retrievals on simulated measurements. In this case this can be done by generating an extinction spectrum with the CDHO and Mie models and then by retrieving the spectral refractive indices with an incorrect set of assumptions in the CDHO and Mie models. However, if this approach is used, one significant source of forward model error is neglected. Because the CDHO model uses symmetric absorption bands, it is unable to model asymmetric absorption features. For infrared extinction by atmospheric aerosols, the most important of these is the OH stretch region between 3500 and 4000 cm^{-1}. Since we have *a priori* knowledge of this feature, an increased forward model error can be included in the affected region manually. This increases the relative weighting of the *a priori* spectrum in this region, allowing a poor fit to the measured spectrum. The retrieved refractive indices in the OH stretch region will therefore be inaccurate, which is probably the greatest weakness of the CDHO model-based retrieval.

The final error term to be included is that due to the uncertainty in the refractive index at an infinite wavelength (m_∞). This introduces another weighting term to the fit between the measurement and the forward model, resulting in the measurement covariance matrix being replaced by the term

$$\mathbf{S}_y = \mathbf{S}_\epsilon + \mathbf{S}_{\mathrm{fm}} + \mathbf{K}_{m_\infty}\mathbf{S}_{m_\infty}\mathbf{K}_{m_\infty}^T, \tag{15}$$

where $\mathbf{K}_{m_\infty}$ is the Jacobian giving the sensitivity of the forward model to the m_∞ parameter, and S_{m_∞} is the covariance matrix for the parameter. In this case, since we are concerned only with a single parameter, K_{m_∞} will actually be a column vector of length m, and S_{m_∞} will be a scalar (the variance of m_∞). Thus the general Eq. (15) can be rewritten as

$$\mathbf{S}_y = \mathbf{S}_\epsilon + \mathbf{S}_{\mathrm{fm}} + \mathbf{k}_{m_\infty}s_{m_\infty}\mathbf{k}_{m_\infty}^T. \tag{16}$$

The vector k_{m_∞} is calculated from an analytical expression for the derivative of β_{ext} with respect to m_∞ each time the forward model is calculated. This matrix then replaces the measurement covariance matrix. The expressions for the retrieval iteration and the cost function, for example, then become

$$\mathbf{x}_{i+1} = \mathbf{x}_i + (\mathbf{S}_a^{-1} + \mathbf{K}_i{}^T\mathbf{S}_y^{-1}\mathbf{K}_i + \gamma\mathbf{D}_n)^{-1}\{\mathbf{K}_i{}^T\mathbf{S}_y^{-1}[\mathbf{y} - \mathbf{f}(\mathbf{x}_i)] - \mathbf{S}_a^{-1}(\mathbf{x}_i - \mathbf{x}_a)\}, \tag{17}$$

(where $\mathbf{D}_n$ is a scaling matrix—the *a priori* covariance matrix in this case) and

$$-2\ln P(\mathbf{x}\,|\,\mathbf{y}) = [\mathbf{y} - \mathbf{f}(\mathbf{x})]^T\mathbf{S}_y^{-1}[\mathbf{y} - \mathbf{f}(\mathbf{x})] + (\mathbf{x} - \mathbf{x}_a)^T\mathbf{S}_a^{-1}(\mathbf{x} - \mathbf{x}_a), \tag{18}$$

respectively. After the final iteration, the covariance matrix of the state (size distribution and band parameters) is given by

$$\hat{\mathbf{S}} = (\mathbf{S}_a^{-1} + \mathbf{K}_i{}^T\mathbf{S}_y^{-1}\mathbf{K}_i)^{-1}. \tag{19}$$

The final step in a retrieval is to calculate the spectral refractive indices and their associated error estimates. The cutdown forward model relating the state to the refractive index [Eq. (12)] has two associated Jacobians: one for the real part of the refractive index, denoted by K_n, and one for the imaginary part, denoted by $\mathbf{K}_k$. These weighting functions allow the calculation of error estimates for the refractive index, with the covariance of n, for example, being given by

$$\mathbf{S}_n = \mathbf{K}_n\hat{\mathbf{S}}_{\tilde{x}}\mathbf{K}_n{}^T, \tag{20}$$

where $\hat{\mathbf{S}}_{\tilde{x}}$ denotes the section of the solution covariance that describes the CDHO bands because the refractive index does not have a functional dependence on the size distribution. In addition, the averaging kernel,

$$A_m = \frac{\partial\mathbf{m}}{\partial\mathbf{x}} \tag{21}$$

can also be calculated, giving the sensitivity of the retrieved refractive index to the state. As with the covariance, this expression is actually two: one each for the real and imaginary parts of the refractive index:

$$\mathbf{A}_n = \mathbf{K}_n\mathbf{A}, \tag{22}$$

$$\mathbf{A}_k = \mathbf{K}_k\mathbf{A}. \tag{23}$$

6. Retrieval with Simulated Measurements

To characterize the performance of the retrieval code, extensive analysis of simulated measurements has been carried out. For such analysis the forward model is used to generate an extinction spectra based on a given set of CDHO band and particle size distribution parameters. This extinction spectra is then used as the measurement vector for a retrieval run in which the *a priori* band parameter set differs from that used to generate the measurement.

Figure 1 shows the spectral fit that results from such a retrieval, where the simulated measurement was generated with a 31-band CDHO model of H_2SO_4–HNO_3–H_2O supercooled ternary solution (STS), and a 24-band model was used for the retrieval. The residuals are shown normalized to the measurement error, which are the error estimates extracted from an actual spectral measurement. Despite the fact that we used a simplified forward model for the retrieval, the spectrum was fitted within the measurement uncertainty for the entire frequency range, except in the OH stretch region. Figure 2 shows both the true and the retrieved refractive-

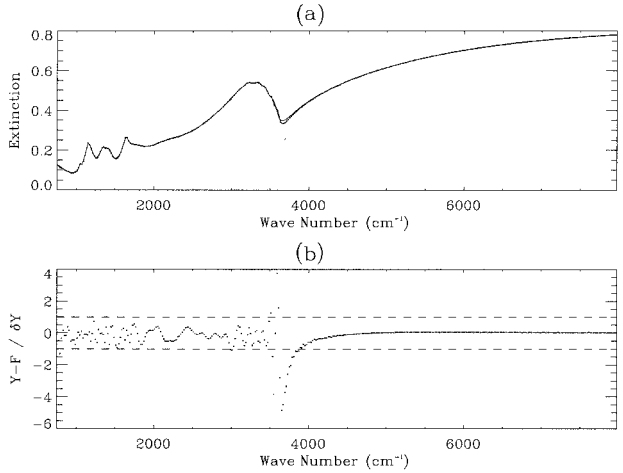

Fig. 1. (a) Simulated extinction spectra generated with the CDHO model (dotted curve) and the corresponding retrieved fit (solid curve). (b) The residuals of the fit normalized to the measurement errors (dotted curve). The dashed lines indicate the 1σ bounds.

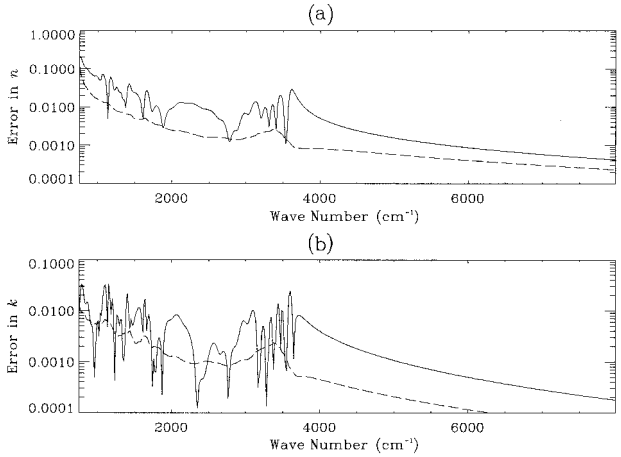

Fig. 3. Absolute difference between the true and the retrieved refractive indices (solid curves) and the retrieved refractive-index error estimates based on measurement errors alone (dashed curves) for the (a) real and (b) imaginary parts.

index spectra corresponding to the fit shown in Fig. 1. The agreement between the two profiles is good for the majority of the spectra; however, Fig. 3 clearly shows that the refractive-index error estimates based on the measurement noise alone grossly underestimate the true discrepancy between the two profiles.

A breakdown of the overall error estimate used in the retrieval, including the forward model and the forward model parameter error, is shown in Fig. 4. It is clear that uncertainties in the forward model are the limiting factors in the precision of the retrieval rather than the measurement error. Figure 5 shows the total error estimates in the refractive indices along with the actual differences between the expected and the retrieved values. Inclusion of the forward model and the forward model parameter error has accounted for the observed discrepancies. These results indicate that we can expect uncertainties to range between approximately 0.001 and 0.1 in the real part of the refractive index and between 10^{-3} and 0.04 in the imaginary part.

7. Retrieval with Measured Extinction Spectra

Spectral measurements of the infrared extinction of $H_2SO_4-HNO_3-H_2O$ STS and $H_2SO_4-H_2O$?>binary solution aerosol have been made at the Molecular Spectroscopy Facility (MSF) at the Rutherford Appleton Laboratory (RAL) as part of the Mapping of Polar Stratospheric Clouds and Ozone Levels Relevant to the Region of Europe (MAPSCORE) project. The RAL MSF uses a 75-dm^3 pressure- and temperature-controlled aerosol cell capable of recreating stratospherically relevant conditions. This is coupled with a Bruker IFS 66v/S Fourier-transform spectrometer,

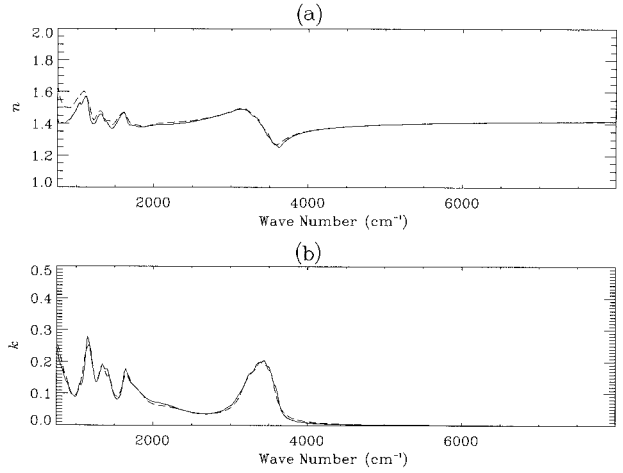

Fig. 2. (a) Real and (b) imaginary refractive indices corresponding to the fit shown in Fig. 1. The solid curves show the true spectra and the dashed curves show the retrieved values.

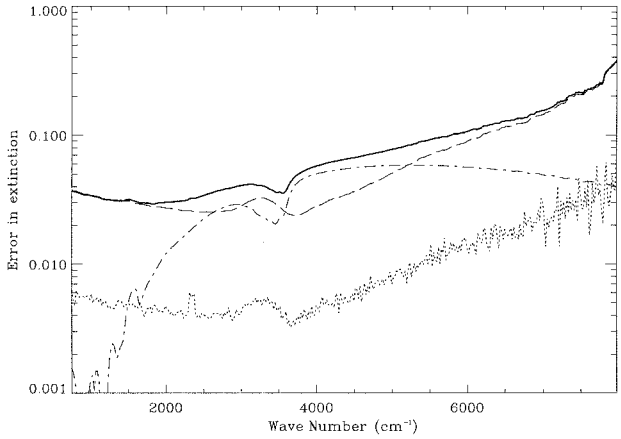

Fig. 4. Full measurement and forward model error estimates used in the retrieval. The dotted curve is the measurement error, the dashed curve is the forward model error (not including that due to the asymmetric OH stretch), the dashed–dotted curve is the forward model parameter error, and the total error is indicated by the heavy solid curve.

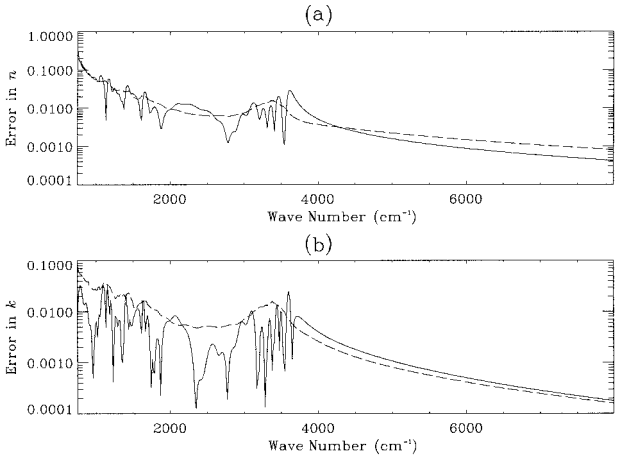

Fig. 5. Same as Fig. 3, except that the dashed curves show the refractive-index uncertainties once the forward model and forward model parameter errors have been taken into account.

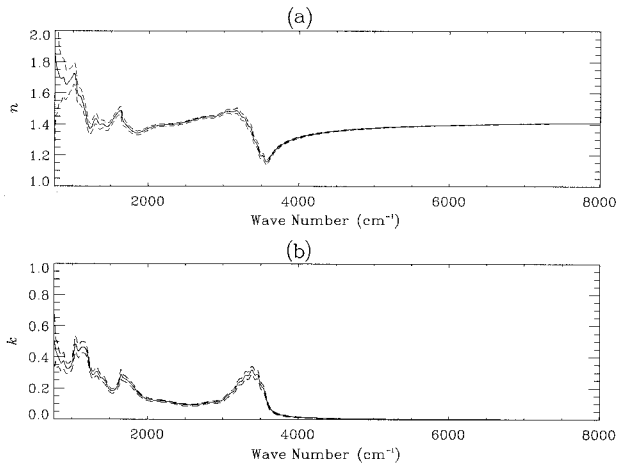

Fig. 7. (a) Real and (b) imaginary refractive indices corresponding to the fit shown in Fig. 6. The dashed curves indicate the 1σ uncertainties.

which is capable of 0.12-cm^{-1} resolution measurements from the near to mid-infrared (350–7000 cm^{-1} when operated with deuterated L-alanine triglycine sulfate and mercury cadmium telluride detectors). The aerosol system is fully described by McPheat *et al.*[17]

Figure 6 shows an example of a STS aerosol spectrum measured at the RAL MSF, as well as the spectral fit given by the retrieval. The spectra, as presented to the retrieval scheme, are the mean of several individual spectra measured over the course of a few minutes. The standard deviation of these individual spectra provide the measurement error estimates for the retrieval. Any cross correlation between measurements (such as might be introduced by apodization by the spectrometer) was neglected in the analysis.

Once again the spectral fit is good, with only the area around the asymmetric OH feature showing any noticeable deviation from the measured spectra. The residuals [Fig. 6(b)], which in this case also take the forward model and forward model parameter uncertainties into account, show that the fit is well within the error bounds. Figure 7 shows the resulting refractive-index spectra, along with their error estimates. In relative terms, the uncertainty in the real part of the refractive index ranges from approximately 10% at the low-frequency end of the spectrum to approximately 0.1% at higher frequencies. The uncertainties on the absorption are relatively higher, ranging between 10% and 20% across the spectrum, mainly due to the low absorption across much of the spectrum.

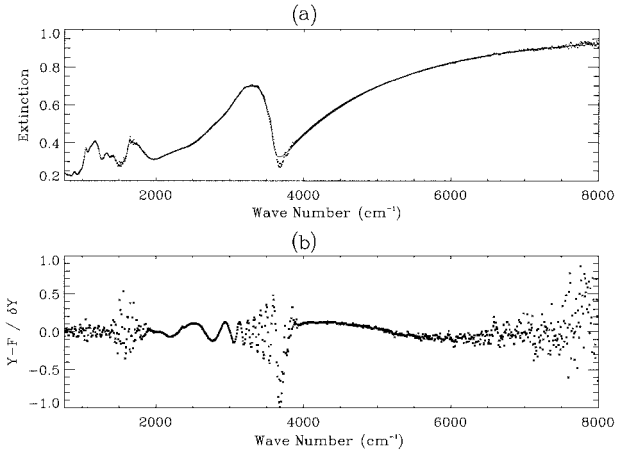

Fig. 6. (a) STS spectra measured at the RAL MSF (points) along with the retrieved spectral fit (solid curve). (b) The residuals, scaled by the total uncertainty (measurement, forward model, and forward model parameter). The aerosol was at a temperature of 250 K, and the retrieved particle size distribution parameters were $N_0 = 1.44 \times 10^6$ cm^{-3}, $r_m = 0.60$ μm, and $S = 1.36$.

Although composition measurements are not available for the data presented here, an initial comparison of this result with published STS refractive indices has been made. The refractive-index measurements of Biermann *et al.*[6] cover a wide range of compositions and temperatures for STS, and software is available that interpolates between the measured values to provide continuous coverage. Using the Biermann *et al.* interpolation routine and the Mie-scattering section of our forward model, we can produce extinction spectra based on the Biermann refractive indices and retrieved particle size distributions from MSF measurements. This facility has been used to compare the Biermann *et al.* refractive indices and those shown in Fig. 7 by performing a simple least-squares fit using a brute-force technique (i.e., stepping through all possible compositions, with steps of 2% concentration by weight in H_2SO_4 and HNO_3, and selecting the one that provides the best fit) between the RAL MSF and Biermann extinction spectra. This procedure has neglected any form of error analysis and is intended only to provide a qualitative comparison between refractive indices produced by the new method and values already in extensive use.

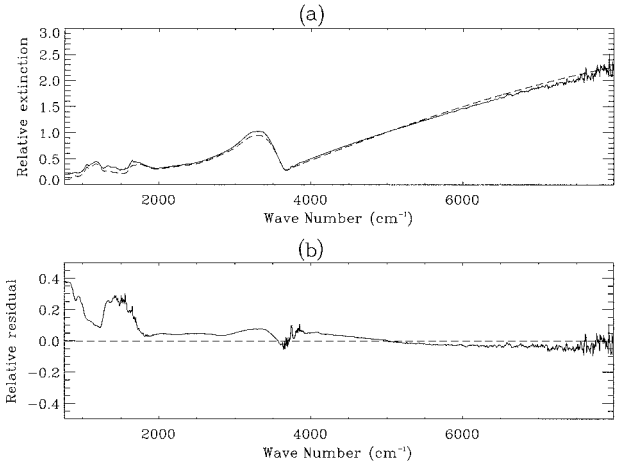

Fig. 8. (a) Comparison of the MSF measured extinction spectrum shown in Fig. 6 (solid curve) and the best fitting modeled spectrum based on the Biermann *et al.* STS refractive database (dashed curve). The relative residuals [(MSF extinction-Biermann extinction)/Biermann extinction] are shown in (b).

The best fit achieved between the Biermann *et al.* data and the RAL MSF measurement shown in Fig. 6 is given in Fig. 8. The Biermann *et al.* spectrum corresponds to a composition of 31-wt.% H_2SO_4 and 5-wt. % HNO_3 by use of the same size distribution as was retrieved for the RAL MSF measurement ($N_0 = 1.44 \times 10^6$ cm^{-3}, $r_m = 0.60$ μm, $S = 1.36$) and the temperature recorded for the MSF measurement, 250 K.

It is clear that, although the extinction spectra share similar absorption features, there are significant differences between them, particularly at small wave numbers. The comparison between the corresponding Biermann *et al.* refractive indices and those derived from the RAL MSF measurements (Fig. 9) shows even more striking differences, with absorption values at low wave numbers being different by up to a factor of 2.

When drawing conclusions from this comparison, care must be taken. Since the composition of the aerosol that produced the extinction spectrum shown in Figs. 6 and 8 is unknown, apart from the fact that it is STS, we cannot be sure we are comparing spectra of similar material. However, it should be noted that this fit was the best for the entire range of the Biermann *et al.* data set. In addition, differences that can be seen in Fig. 8 are consistent with those found between RAL MSF spectra and synthetic spectra based on the Biermann *et al.* data reported by McPheat *et al.*,[9] where discrepancies of over 20% in extinction were also found below 2000 cm^{-1}. Wagner *et al.*[8] also find similarly sized discrepancies among the Biermann data set binary H_2SO_4 or HNO_3 solutions; their own measurements; and the refractive-index data of Tisdale *et al.*,[2] Niedziela *et al.*,[3] Norman *et al.*,[4] and Myhre *et al.*[5]

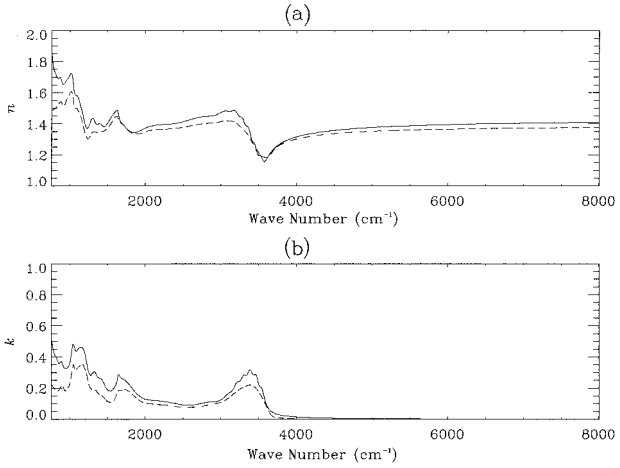

Fig. 9. Comparison between the refractive indices derived from the MSF extinction spectrum shown in Figs. 6 and 8 (solid curve) and the Biermann *et al.* refractive indices corresponding to the extinction spectrum shown in Fig. 8. Again, (a) shows the real part of the refractive index and (b) the imaginary part.

8. Future Research

There are three areas that need to be addressed for the analysis technique presented here to realize its full potential. The first of these is the inability of the CDHO model to represent asymmetric absorption features. It is hoped that by the inclusion of an asymmetry parameter (essentially introducing a directional dependence to the damping constant γ_j in selected bands) this problem can be overcome.

The other two issues relate to the measurements used in conjunction with this analysis technique. It is highly desirable that independent measurements of the particle size distribution and m_∞ be made, as well as the measurements of the extinction spectra and particle composition. A better definition of these two quantities will result in a more accurate and stable retrieval because it will better constrain the solution. In addition, a direct measurement of the particle size distribution will allow the correct form of distribution to be used in the retrieval.

Once these issues have been addressed, and extinction spectra of aerosol of a known (and atmospherically relevant) composition are available, an extensive database of atmospheric aerosol refractive indices can be built up. With such a resource the accuracy of remotely measured aerosol properties can be substantially improved, both by reanalysis of existing data and by application to new measurements.

9. Conclusion

A new algorithm has been developed to retrieve spectral refractive indices, along with the parameters of the particle size distribution, from infrared extinction spectra of aerosol. The algorithm makes use of a classical damped harmonic-oscillator (CDHO) model of molecular absorption and a Mie-scattering model of aerosol extinction. The primary advantage of this technique over the Kramers–Kronig-based methods usually used to analyze such measurements is that it allows the determination of both the real and the

imaginary parts of the refractive index, at full spectral resolution, from a single extinction spectrum.

Extensive characterization of the forward model and the retrieval scheme has been carried out. It has been determined that at present the uncertainty in the result is limited by the uncertainties in the refractive-index anchor value (m_∞) and forward model error. The forward model error has three main sources: (i) the uncertainty in the number of absorption bands required for the CDHO model, (ii) the inability to model asymmetric absorption features (primarily the OH stretch region around 3500 cm^{-1}) with the symmetric absorption bands of the CDHO model, and (iii) poor prior knowledge of the particle size distribution. It is hoped that the symmetry limitation can be overcome by the introduction of an asymmetry term in the CDHO model; however, the other limitations can be overcome only by simultaneous measurements of m_∞ and the particle size distribution with the aerosol extinction spectra.

The new retrieval scheme has been applied to measurements of supercooled ternary solution (STS) aerosol measured at the Molecular Spectroscopy Facility at the Rutherford Appleton Laboratory. The CDHO model was able to provide a good fit to the measured spectrum, and well-defined refractive indices were obtained. These results have been compared with values from the Biermann *et al.*[6] measurements of thin-film STS by finding the best fit between the RAL MSF spectrum and a modeled extinction spectrum by use of the Biermann refractive indices. This comparison has revealed significant differences in both the extinction and the refractive-index spectra, which are similar to differences found by other authors in comparisons with other data sets and the Biermann *et al.* values.

Appendix A: Analytical Derivatives of the Forward Model

Derivatives of the forward model with respect to the parameters of the size distribution can be obtained directly from Eq. (11)[16]:

$$\frac{\partial \beta^{\text{ext}}}{\partial N_0} = \frac{1}{\ln S}\sqrt{\frac{\pi}{2}}\int_0^\infty rQ^{\text{ext}} \exp\left[-\frac{(\ln r - \ln r_m)^2}{2\ln^2 S}\right]dr, \tag{A1}$$

$$\frac{\partial \beta^{\text{ext}}}{\partial r_m} = \frac{N_0}{\ln^3 S}\frac{1}{r_m}\sqrt{\frac{\pi}{2}}\int_0^\infty rQ^{\text{ext}}(\ln r - \ln r_m)\exp \times\left[-\frac{(\ln r - \ln r_m)^2}{2\ln^2 S}\right]dr, \tag{A2}$$

$$\frac{\partial \beta^{\text{ext}}}{\partial S} = \frac{N_0}{S\ln^2 S}\sqrt{\frac{\pi}{2}}\left\{\frac{2}{\ln^2 S}\int_0^\infty rQ^{\text{ext}}(\ln r - \ln r_m)^2 \exp\left[-\frac{(\ln r - \ln r_m)^2}{2\ln^2 S}\right]dr - \int_0^\infty rQ^{\text{ext}}\exp\left[-\frac{(\ln r - \ln r_m)^2}{2\ln^2 S}\right]dr\right\}. \tag{A3}$$

Grainger *et al.*[16] give expressions for the derivatives of the extinction with respect to the refractive index, $\partial\beta^{\text{ext}}/\partial n$ and $\partial\beta^{\text{ext}}/\partial k$ (omitted here for brevity). In turn, the derivatives of refractive index with respect to the dielectric quantities ϵ' and ϵ'' are

$$\frac{\partial n}{\partial \epsilon'} = \frac{\epsilon'}{\{8[(\epsilon'^2+\epsilon''^2)^{1/2}+\epsilon'](\epsilon'^2+\epsilon''^2)\}^{1/2}} + \frac{1}{\{8[(\epsilon'^2+\epsilon''^2)^{1/2}]\}^{1/2}}, \tag{A4}$$

$$\frac{\partial n}{\partial \epsilon''} = \frac{\epsilon''}{\{8[(\epsilon'^2+\epsilon''^2)^{1/2}+\epsilon'](\epsilon'^2+\epsilon''^2)\}^{1/2}}, \tag{A5}$$

$$\frac{\partial k}{\partial \epsilon'} = \frac{\epsilon'}{\{8[(\epsilon'^2+\epsilon''^2)^{1/2}-\epsilon'](\epsilon'^2+\epsilon''^2)\}^{1/2}} - \frac{1}{\{8[(\epsilon'^2+\epsilon''^2)^{1/2}]\}^{1/2}}, \tag{A6}$$

$$\frac{\partial k}{\partial \epsilon''} = \frac{\epsilon''}{\{8[(\epsilon'^2+\epsilon''^2)^{1/2}-\epsilon'](\epsilon'^2+\epsilon''^2)\}^{1/2}}. \tag{A7}$$

The derivatives of ϵ' and ϵ'' with respect to the band parameters are

$$\frac{\partial \epsilon'}{\partial \nu_j} = \frac{2S_j\nu_j}{(\nu_j^2-\nu^2)^2+\gamma_j^2\nu^2} - \frac{4S_j\nu_j(\nu_j^2-\nu^2)^2}{[(\nu_j^2-\nu^2)^2+\gamma_j^2\nu^2]^2}, \tag{A8}$$

$$\frac{\partial \epsilon''}{\partial \nu_j} = \frac{-4S_j\gamma_j\nu(\nu_j^2-\nu^2)}{[(\nu_j^2-\nu^2)^2+\gamma_j^2\nu^2]^2}, \tag{A9}$$

$$\frac{\partial \epsilon'}{\partial \gamma_j} = \frac{-2S_j(\nu_j^2-\nu^2)\gamma_j\nu^2}{[(\nu_j^2-\nu^2)^2+\gamma_j^2\nu^2]^2}, \tag{A10}$$

$$\frac{\partial \epsilon''}{\partial \gamma_j} = \frac{S_j\nu}{(\nu_j^2-\nu^2)^2+\gamma_j^2\nu^2} - \frac{2S_j\gamma_j^2\nu^3}{[(\nu_j^2-\nu^2)^2+\gamma_j^2\nu^2]^2}, \tag{A11}$$

$$\frac{\partial \epsilon'}{\partial S_j} = \frac{(\nu_j^2-\nu^2)}{(\nu_j^2-\nu^2)^2+\gamma_j^2\nu^2}, \tag{A12}$$

$$\frac{\partial \epsilon''}{\partial S_j} = \frac{\gamma_j\nu}{(\nu_j^2-\nu^2)^2+\gamma_j^2\nu^2}. \tag{A13}$$

We can combine these expressions to give the deriv-

atives of the extinction with respect to the band parameters using the chain rule:

$$\frac{\partial \beta^{\text{ext}}}{\partial Z} = \frac{\partial \beta^{\text{ext}}}{\partial n}\frac{\partial n}{\partial Z} + \frac{\partial \beta^{\text{ext}}}{\partial k}\frac{\partial k}{\partial Z} = \frac{\partial \beta^{\text{ext}}}{\partial n}\left(\frac{\partial n}{\partial \epsilon'}\frac{\partial \epsilon'}{\partial Z} + \frac{\partial n}{\partial \epsilon''}\frac{\partial \epsilon''}{\partial Z}\right) + \frac{\partial \beta^{\text{ext}}}{\partial k}\left(\frac{\partial k}{\partial \epsilon'}\frac{\partial \epsilon'}{\partial Z} + \frac{\partial k}{\partial \epsilon''}\right), \tag{A14}$$

where Z represents one of ν_j, γ_j, or S_j.

We acknowledge funding from the European Union Framework 5 project particles in the upper troposphere and lower stratosphere and their role in the climate system (EVK2-CT-2001-00112) and the United Kingdom Natural Environment Research Council's Core Strategic Measurements for Atmospheric Science for funding this research. Thanks also to Robert McPheat at the RAL MSF for providing the aerosol extinction spectra used in developing the retrieval scheme.

References

1. Intergovernmental Panel on Climate Change, *IPCC Third Assessment Report: Climate Change 2001* (Cambridge U. Press, London, 2001).
2. R. T. Tisdale, D. L. Glandorf, M. A. Tolbert, and O. B. Toon, "Infrared optical constants of low-temperature H_2SO_4 solutions representative of stratospheric sulfate aerosols," J. Geophys. Res. **103,** 25353–25370 (1998).
3. R. F. Niedziela, M. L. Norman, C. L. DeForest, R. E. Miller, and D. R. Worsnop, "Temperature and frequency-dependent study of H_2SO_4 aerosol optical constants using Fourier transform and tunable diode laser infrared spectroscopy," J. Phys. Chem. A **103,** 8030–8040 (1999).
4. M. L. Norman, J. Qian, R. E. Miller, and D. R. Worsnop, "Infrared complex refractive indices of supercooled HNO_3/H_2O aerosols," J. Geophys. Res. **104,** 30571–30584 (1999).
5. C. E. L. Myhre, D. H. Christensen, F. M. Nicolaisen, and C. J. Nielsen, "Spectroscopic study of aqueous H_2SO_4 at different temperatures and compositions: variations in dissociation and optical properties," J. Phys. Chem. A **107,** 1979–1991, doi: 10.1021/jp026576n (2003).
6. U. M. Biermann, B. P. Luo, and T. Peter, "Absorption spectra and optical constants of binary and ternary solutions of H_2SO_4, HNO_3, and H_2O in the mid infrared at atmospheric temperatures," J. Phys. Chem. A **104,** 783–793 (2000).
7. M. L. Norman, R. E. Miller, and D. R. Worsnop, "Ternary $H_2SO_4/HNO_3/H_2O$ optical constants: new measurements from aerosol spectroscopy under stratospheric conditions," J. Phys. Chem. A **106,** 6075–6083 (2002).
8. R. Wagner, A. Mangold, O. Möhler, H. Saathoff, M. Schnaiter, and U. Schurath, "A quantitative test of infrared optical constants for supercooled sulphuric and nitric acid droplet aerosols," Atmos. Chem. Phys. **3,** 1147–1164 (2003).
9. R. A. McPheat, S. F. Bass, D. A. Newnham, J. Ballard, and J. J. Remedios, "Comparison of aerosol and thin film spectra of supercooled ternary solution aerosol," J. Geophys. Res. **107,** doi:10.1029/2001JD000641 (2002).
10. M. L. Clapp, R. E. Miller, and D. R. Worsnop, "Frequency-dependant optical constants of water ice obtained directly from aerosol extinction spectra," J. Phys. Chem. **99,** 6317–6326 (1995).
11. S. F. Bass, "Optical properties of laboratory-generated polar stratospheric cloud particles," D.Phil. thesis (University of Oxford, Oxford, UK, 2003).
12. J. E. Bertie, S. L. Zhang, and C. D. Keefe, "Infrared intensities of liquids XVI. Accurate determination of molecular band intensities from infrared refractive index and dielectric constant spectra," J. Mol. Struct. **324,** 157–176 (1994).
13. W. H. Press, S. Teukolksy, W. T. Vetterling, and B. Flannery, *Numerical Recipes in C: The Art of Scientific Computing, 2nd ed.* (Cambridge U. Press, Cambridge, UK, 1995).
14. C. D. Rodgers, *Inverse Methods for Atmospheric Sounding: Theory and Practice* (World Scientific, London, 2000).
15. M. J. Dignam, "Fourier-transform polarization spectroscopy," Appl. Spectrosc. Rev. **24,** 99–135 (1988).
16. R. G. Grainger, J. Lucas, G. E. Thomas, and G. B. L. Ewen, "Calculation of Mie derivatives," Appl. Opt. **43,** 5386–5393 (2004).
17. R. A. McPheat, D. A. Newnham, R. G. Williams, and J. Ballard, "Large-volume, coolable spectroscopic cell for aerosol studies," Appl. Opt. **40,** 6581–6586 (2001).